

PAPER • OPEN ACCESS

Simulation and Optimization of a Metallic Ferry under MLC70 Loading

To cite this article: Mohamed N. Lotfy *et al* 2020 *IOP Conf. Ser.: Mater. Sci. Eng.* **974** 012008

View the [article online](#) for updates and enhancements.

You may also like

- [The Effectiveness of Palembang Ferry Port Displacement](#)
Rhaptalyani Herno Della and Taih-Cherng Lirn
- [Interference and interactions in open quantum dots](#)
J P Bird, R Akis, D K Ferry et al.
- [Analysis of Systemic Safety Issues in Domestic RoRo Ferry Port Operation Using the Concept of Safety-II](#)
A Nurwahyudy, T Pitana and S Nugroho



245th ECS Meeting
San Francisco, CA
May 26–30, 2024

PRiME 2024
Honolulu, Hawaii
October 6–11, 2024

Bringing together industry, researchers, and government across 50 symposia in electrochemistry and solid state science and technology

Learn more about ECS Meetings at
<http://www.electrochem.org/upcoming-meetings>

 Save the Dates for future ECS Meetings!

Military Technical College
Kobry El-Kobbah,
Cairo, Egypt



13th International Conference
on Civil and Architecture
Engineering
ICCAE-13-2020

Simulation and Optimization of a Metallic Ferry under MLC70 Loading

Mohamed N. Lofly¹, Yasser A. Khalifa¹, Abdelrahim k. Dessouki² and Elsayed Fathallah¹

¹Department of Civil Engineering, Military Technical College, Cairo, Egypt.

²Ain Shams University, Cairo, Egypt.

Abstract. Floating ferries are used for both civilian and military purposes. This study concerned with a ferry composed of sixteen connected floating pontoons. This ferry is simulated and optimized to carry Military Load Capacity MLC70 (Tank load). Consequently to the increasing demand of evolution and cost optimization, the design optimization is performed in this paper to obtain the optimum minimum weight which minimizes both the cost and the buoyancy factor. The simulation of the ferry is performed using the finite element program ANSYS software. Furthermore, different grades of the structural steel, hybrid materials (steel stiffeners covered with aluminium plates) and aluminium alloy are incorporated in this study. This simulation is verified with both practical and mathematical results. The performance of the ferry is investigated. In addition to the design parameters, constraints and objective functions are determined. The optimum weight of the ferry is obtained, followed by a reduction in the buoyancy factor; accordingly the capacity of the ferry can be increased. Comparison between the behaviour of the different ferries using different materials is operated considering stresses, deformations and weight. Conclusions and recommendations are then stated.

Keywords: Floating; Pontoon; Optimization; Ferry; Steel; Aluminium; Modelling; ANSYS

1. Introduction

Transport is of vital importance in the flexibility of traffic and the affluence of the economy, delivering people, goods and vehicles from one place to another. The usage of floating bridges is essential when facing relatively deep water obstacles. Floating bridges usage can be dated back to 2000 BC. [1]. The floating bridges are used in peace and war times as they have a great importance in emergency situations. There are many types of floating bridges according to the conditions of the site to be constructed in and according to the types of obstacles to cross [2]. The most common types of the floating bridges are the continuous pontoon floating bridge and the discrete pontoon floating bridge [3, 4]. There are two main features that judge the efficiency of the pontoon bridges; the safety and the speed of erection over the obstacles [5]. As a result of the great need to the usage of the floating



bridges, many upgrades and develops are being applied to the floating bridges. Many researchers interested in studying floating bridges using analytical and numerical methods in a companion with software programs. At the beginning of the modelling of the floating pontoon bridges many simplifications are applied to be able to simulate the required models with the available software programs. First they considered the pontoon as a beam rested on an elastic foundations and subjected to the applied loads [6]. Shahrabi et al. [7] developed a method to analyze the motions of a floating pier which was represented as number of floating pontoons. These floating pontoons were simulated as rigid bodies and connected to each other's by rigid and flexible connectors. After that, the development of the finite element programming resulted in the complete simulation of the models. Khalifa et al. [8] studied the performance of the floating bridges under longitudinal and transverse eccentric static load using ANSYS. Fu and Cui [9], numerically studied the effect of the dynamic and the static loading on the hydro elastic responses of connected pontoons and introduced a numerical method for analysis of a ribbon floating bridge [10]. Sun et al. [11] studied the dynamic response of a floating bridge which was consisting of multi-modules. They determined the bending moment and the mooring force of the floating bridge. Zhang et al. [3] investigated the dynamic response of two analytical models for the two types of pontoon bridges subjected to moving loads for different depths of water. They concluded that the water depth has a little effect on the dynamic responses of floating bridges. Hirono et al. [12] divided the floating bridge to floating units and developed a measurement system to determine the vertical displacement of these floating units to determine the displacement of the floating bridge under the applied loads. The design of floating bridges to meet the requirements with an economic cost is a new challenging issue. The floating bridges design must consider several environmental loads such as waves, wind and current loads [13]. These loads in addition to the applied loads from the carried vehicles must be investigated and analyzed very carefully. Cheng et al. [13] studied the effect of the environmental loads. Halvor et al. [14] investigated the floating bridges under the same environmental loads and presented a numerical solution to get the required stresses, deformations and moments. Sha et al. [15] studied the dynamic response of the floating bridges under these environmental loads.

2. Optimization

Economic design of structures without exceeding the constraints is a challenge for the designers. Optimization is defined as doing something or design something as well as possible [16]. There are many techniques of optimization which is differing in applications, advantages and disadvantages. The development of optimization techniques and optimization software programs are in a continuous increase. Genetic Algorithms are used in many optimization experiments with different techniques a long time ago. These genetic algorithms are used for the single objective optimization experiments at the first, and then they are expanded to deal with multi-objective optimization. Pareto genetic algorithm is a developed technique that can deal with the multi-objective optimization experiments depending on the weight factor of variables to get the optimum solution as well as possible [17]. Pareto optimization technique is used till our moment due to its advantage of showing the best desired solution with a great weight factor from many other solutions [18, 19]. The researchers and designers continued their development in such a challenging topic and applied many developed optimization techniques to many structures. In 1989 Torn et al [20] presented a guide book that explained the global optimization and introduced examples of many optimization problems and how to get the proper technique of the optimization and the solution of the problem. Carlos and Coello [21] made a comprehensive survey of evolutionary-based multi-objective optimization techniques. Koumouis and Arsenis [22] performed a detailed optimization design of reinforced concrete members of a multi-story building. Hong and Adeli [23] studied the genetic algorithm optimization which was applied by binary representation of parameters. They used floating-point genetic algorithm in studying the cost optimization of composite floors to get rid of the disadvantages of the binary method. Philippe Rigoo and Claude Fleury [24] used the Stiffened panels software as a development of a new methodology to determine the preliminary design of floating hydraulic structures and naval structures. They presented an algorithm for optimization based on convex linearization. Mehdi and Aidini [25] defined the optimum mooring systems. They used a genetic algorithm for the optimization of the design of

mooring platforms and presented new procedures to solve these floating structures in a quick way to get the best mooring system. Matthias et al [26] presented a new tool of optimization for mooring systems for floating structures foundations. They used MATLAB in their optimization experiments. Fathallah et al [27, 28] applied optimization for a composite submerged hull composed of composite layers with different layers orientations. Their objective function was to minimize the buoyancy factor by using ANSYS. Brittani R. Russell et al [29] developed the characteristics of the deployable floating causeways due to the increasing need to this type of bridges. They studied the reconceptualization and the optimization of floating causeways.

In this study, the steel ferry is simulated and optimized to achieve the minimum weight for the ferry using finite element modelling by ANSYS software. Additionally, different grades of the structural steel, hybrid materials (steel and aluminium) and aluminium alloy are incorporated in this study.

3. Model definition

3.1. Geometry

The studied floating ferry is analysed to carry the Military Load Capacity MLC-70 (Tank load). It is composed of sixteen floating pontoons connected together. Each pontoon is composed of upper deck, lower deck and round side sheets. These sheets are modelled as shell elements, which are supported by internal stiffeners in vertical, longitudinal and transverse directions with different cross sections. These stiffeners are designed as beam elements. The pontoon's dimensions and characteristics are illustrated in **Table 1**. The pontoon is simulated in finite element program ANSYS shown in Figure 1

Table 1: The floating pontoon dimensions and characteristics

Length	5.25m
Width	2.4 m
Depth	1.5 m
Weight	3.356 ton

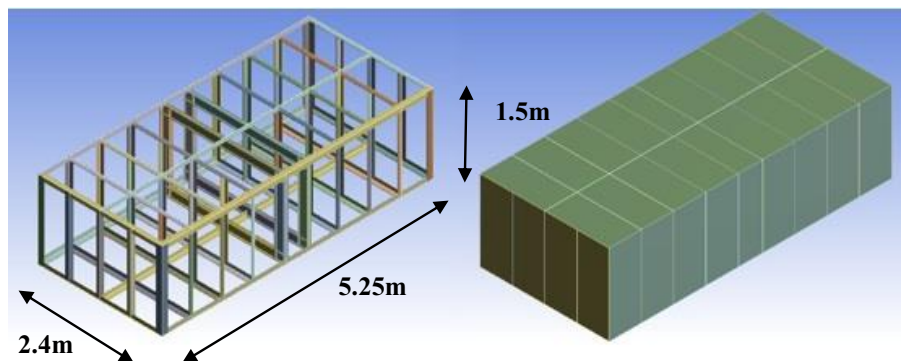


Figure 1: The Isometric view of the floating pontoon.

These floating pontoons are made of steel 37 with properties illustrated in **Table 2**[8, 30].

Table 2: The properties of structural steel

Density	7850 kg/m ³
Tensile yield strength	2.4 × 10 ⁸ (Pa)

Compressive yield strength	2.4×10^8 (Pa)
Tensile ultimate strength	3.6×10^8 (Pa)

The ferry is composed of sixteen floating pontoon with a total length of (21.3 m), a total width of (9.9 m) and a depth of (1.5 m). These pontoons are arranged as follows in **Figure 2**; four pontoons in the transverse direction are separated by 10 cm and these pontoons are repeated another three times in the longitudinal direction.

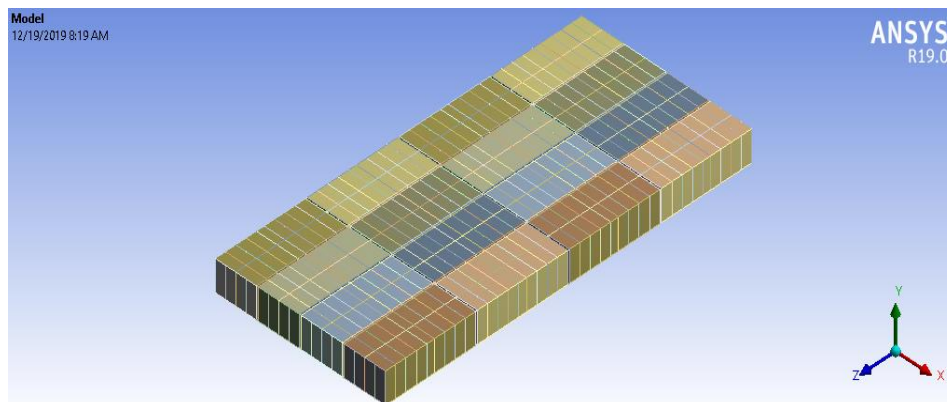


Figure 2: The floating ferry

These pontoons are connected together by upper and lower connections. The connection system between pontoons is simulated to be 8 connections at the long directions divided on the upper and the lower levels and 6 connections in the short direction also, divided also on the upper and the lower levels. The characteristics of the ferry are as shown in **Table 3**.

Table 3: The dimension of the floating ferry

Length	21.3 m
Width	9.9 m
Depth	1.5 m
Weight	53698 Kg

3.2. Loads

The applied load is the load of the tank MLC70 and the characteristics of the tank are as shown in **Table 4**.

Table 4: The floating ferry properties

Tank weight (W)	63.5 ton
Track length (L)	4.5 m
Track width (B)	0.5 m

The pressure from the tank tracks over the ferry (P) is calculated as:

$$P = \frac{W}{2 * L * B} \quad (1)$$

3.3. Boundary conditions

As shown in **Figure 3** the ferry is subjected to the tank load simulated as the two paths illustrated in red colour. The own weight of the ferry is taken into consideration. The elastic supports are assigned to the lower deck to represent the effect of the water, using calculated specific elastic stiffness (K).

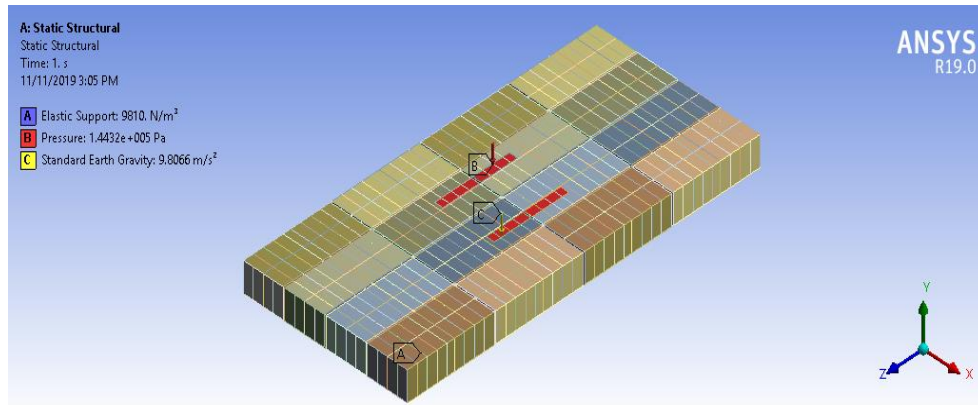


Figure 3: The boundary conditions

Following the principles of floating; the weight of the ferry is equal to the weight of the displaced volume of water by the ferry[31]. The stiffness of the elastic supports differs from one case to another according to the density of the fluid, the stiffness of the submerged structure and its mass.

3.4. Elastic support stiffness calculation

In this model the lower deck of the ferry is supported with elastic supports with stiffness (K) so,

$$F_w = w_w \quad (2)$$

Where, (F_w) represents the weight of the ferry, and (w_w) represents the weight of the displaced water. The own weight of the steel ferry (F_w) is calculated using ANSYS software and (w_w) must be equal to that weight to keep the ferry floating. The weight of the displaced water is computed as follows:

$$w_w = F_b \times F_L \times \Delta \times \gamma_w \quad (3)$$

Where, (F_b) represents the breadth of the ferry without connections = 9.6 (m), (F_L) represents the length of the ferry without connections = 21 (m), (Δ) represents the draft of the ferry under its own weight, (γ_w) represents the density of water = 1000 (kg/m³)

By substituting in equation (3), (Δ) is calculated. The stiffness of the elastic support (K) must make the deformation of the ferry under its own weight equal to (Δ). The stiffness is computed as follows:

$$w_w = k \times F_b \times F_L \times \Delta \quad (4)$$

By substituting in equations (3) and (4).

$$k = \gamma_w \quad (5)$$

4. Validation

The draft of the ferry from the simulation by ANSYS software is compared to the practical and mathematical results. The practical result is shown in **Figure 4**, showing the draft of the ferry under its own weight. The draft of the ferry under its own weight measured to be (26.8 cm) from field.



Figure 4: The practical value of the draft of the steel ferry

Using mathematical equations, the draft is determined as follows:

$$F_w = w_w \quad (6)$$

The own weight of the steel ferry equals (53698 Kg), so w_w must be equal to that weight to keep the ferry floating.

$$w_w = F_b \times F_L \times \Delta \times \gamma_w = F_w \quad (7)$$

$$\Delta = \frac{F_w}{F_b \times F_L \times \gamma_w} \quad (8)$$

By substituting in equation (8), (Δ) is calculated to be (26.59 cm). The numerical results from the simulation in ANSYS are based on the mathematical equations therefore; the results are the same as shown in **Figure 5** and matches with the practical results with a matching percentage of (99.2%).

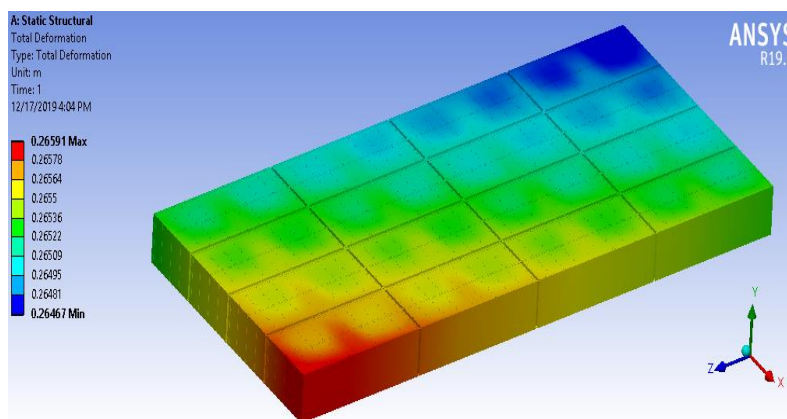


Figure 5: The draft of the ferry under its own weight

5. Simulation of the ferry

5.1. Beam and shell elements simulation

The simulation of the ferry begins with determining the coordinates of every member. These coordinates are simulated as the key points in the graphical user interface of the software program. The stiffeners of the pontoon are simulated as beam elements. There are five different cross sections for the beam elements used in this model. On the other hand, the upper, lower and rounded side sheets are simulated as shell elements which are created from edges with the required thicknesses. After that, the pontoon is repeated by generating two patterns; the first pattern repeats the finished pontoon in the X direction another three times to get the required four pontoons. The second pattern repeats these four pontoons in the Z direction another three times to get the required ferry which is composed of 16 floating pontoons as shown in **Figure 2**.

5.2. Elements contact

The elements are now generated, but still work individually, therefore the elements must be connected together. To connect the elements there are a target and contact bodies. The shell elements are considered the target and the beam elements (stiffeners) are considered the contact bodies.

5.3. Meshing

The smaller the element size is the more accurate the results are, but also it takes more time in solving the model. The smart meshing with different elements sizes is performed more than one time until the results have almost the same values. The meshing is refined at the critical position (tank tracks and the deck of the ferry around the tank tracks) to get more accurate results as shown in **Figure 6**.

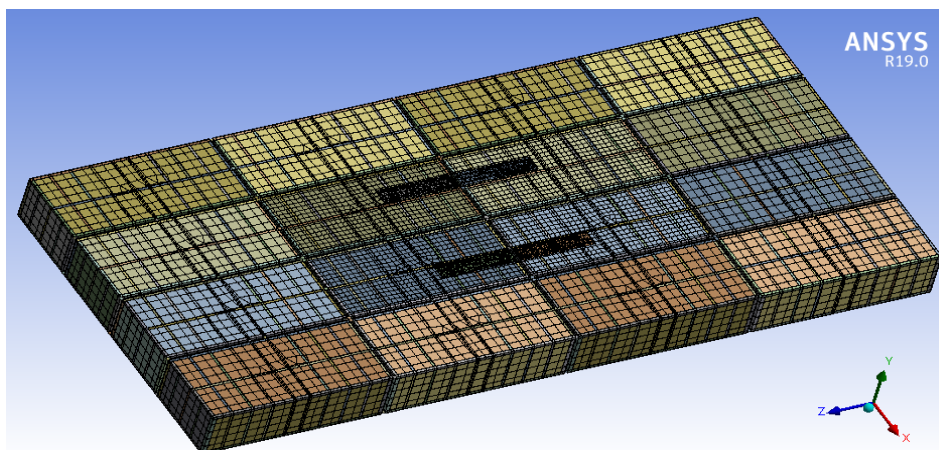


Figure 6: The meshing of the ferry

5.4. Solution

The analysis is performed according to the previous simulation and the required results are determined. The total deformation and Von Misses stresses are tabulated in **Table 5**.

Table 5: The results of the ferry under MLC70

Total deformation	0.59407 m
Von Misses stresses	8.7215×10^7 Pa

Figure 7 shows that the total deformation of the ferry under the static load of MLC70 is symmetric with a maximum value of (0.594 m).

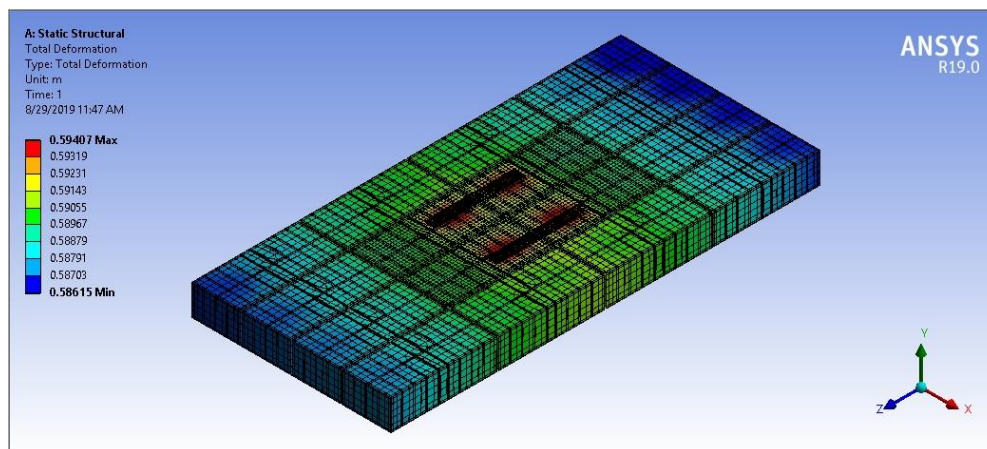


Figure 7: The total deformation of the ferry under MLC70

Figure 8 illustrates the Von Mises stresses. The ferry is affected by a symmetric manner of the stresses over the ferry under the load of the MLC70 with a maximum value at the tank tracks. The connections between the pontoons are affected by these applied loads, specially the transverse connections. The maximum value is $(8.7215 \times 10^7 \text{ Pa})$.

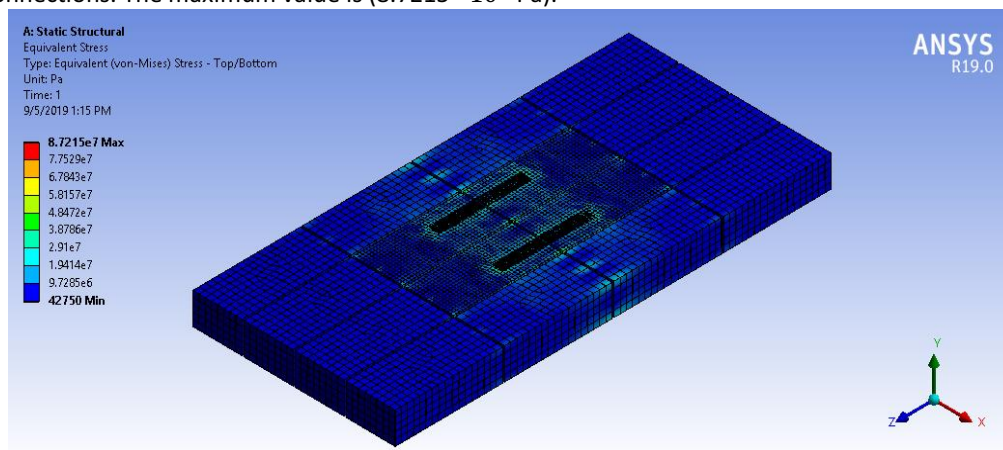


Figure 8: The von-Mises stresses under MLC70

6. Optimization Process

There are many techniques of optimization and many are supported by ANSYS such as screening, multi-objective genetic algorithm, non-dominated sorting genetic algorithm (NSGA), non-linear programming by quadratic lagrangian, etc. According to the number and type of input parameters the used technique is determined automatically [32]. In our study the screening optimization is used to get the optimum weight of the ferry as well as possible as a rapid process. The Screening optimization method uses a simple approach based on sampling and sorting. This method supports multiple objectives and constraints as well as all types of input parameters. The screening method is the first process that is used in the new developed optimization strategy which is called the multiphase optimization strategy (MOST)[33, 34]. Usually, it is used for preliminary design, which may lead the designers to reach to the predicted results in a quick way instead of try and error methods. This flow chart illustrate the used technique to get the optimum design.

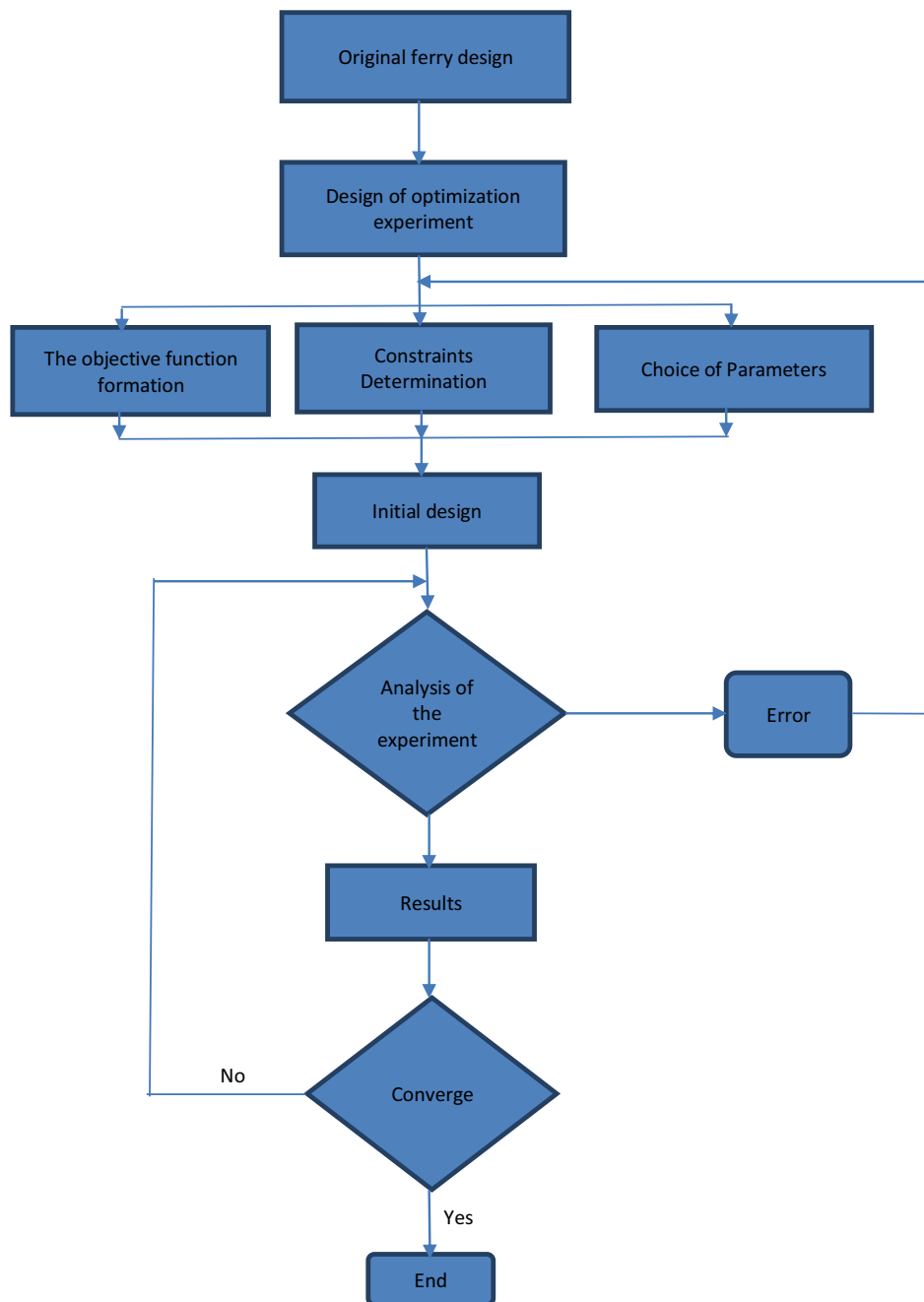


Figure 9: Optimization Flow Chart

6.1. Objective function

In order to apply the optimization process to the ferry, it is obligatory to determine in advance the objective function to be able to determine the parameters and the constraints. In this study, the optimization is performed at two stages; the cross sections are optimized first, then the shell thicknesses in the second stage. The objective function is to minimize the buoyancy factor (B F) that

results in the reduction of the ferry weight. The following equation defines the buoyancy factor [27, 35-37].

$$\text{The buoyancy factor (B F)} = \frac{W_t}{V_t \times \gamma_w} \quad (9)$$

Where, (W_t) represents the total weight of the structure and (V_t) represents the total volume of the structure. Hence, the objective function is to minimize the buoyancy factor. Therefore, the objective function is defined as:

$$F_1(X): \text{minimize } B F = \frac{W_t}{V_t \times \gamma_w} \quad (10)$$

6.2. Constraints

The optimization problem is constrained under two constraints; the stress constraint (g_1) and the deformation constraint (g_2) which are defined as follows:

$$g_1 = \frac{f_{act}}{f_y} \leq 1 \quad (11)$$

$$g_2 = \frac{\Delta}{D_t} \leq 0.8 \quad (12)$$

Where, (f_{act}) represents the actual stress from the applied loads and (f_y) represents the strength of the materials which equals (2.4 t/cm²) for steel 37.

6.3. Design variables

The design variables are the parameters, which are supposed to be optimized. These parameters are the cross section dimensions of the three angles sections (angle 80, angle 90 and angle 120) and two I-beams sections (I-beam 160 and I-beam 180).

$$W_i^L \leq W_i \leq W_i^u, \quad i=1,2,\dots,6 \quad (13)$$

Where, (W_i) represents the cross sections of the angles (the 2 legs dimensions) for every angle (angle 80, angle 90 and angle 120) respectively, (W_i^L) represents the lower bound value for every parameter and (W_i^u) represents the upper bound value.

$$W_{fi}^L \leq W_{fi} \leq W_{fi}^u, \quad i=1,2,3,4 \quad (14)$$

Where, (W_{fi}) represents the flanges of the two I-beams (lower flanges, then upper flanges) respectively, (W_{fi}^L) represents the lower bound and (W_{fi}^u) represents the upper bound.

$$W_h^L \leq W_h \leq W_h^u, \quad i=1,2 \quad (15)$$

Where, (W_h) is the height of the two I-beams (I-beam 160 and I-beam 180) respectively, (W_h^L) represents the lower bound and (W_h^u) represents the upper bound. These parameters are optimized together with a thousand trial for each parameter to reach the optimum solution as well as possible. Every parameter results are determined through the optimization process and these results are chosen to be convergent to the objective function within the limits of the constraints. The results have a theoretical value that are not easy to be manufactured, but these values may be rounded to the values that can be manufactured.

7. Results

The results are generated from the chosen samples composing a thousand result of the optimization process as shown in **Figure 10**.

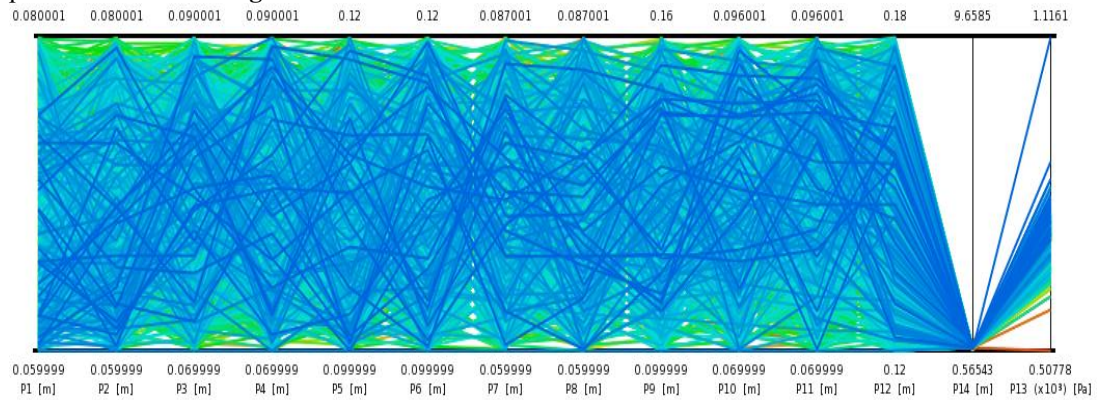


Figure 10: The whole optimization results

According to the design of the experiment these are the best three candidate results which are the most approached results to the optimum result. These candidate points achieve the objective function without exceeding the constraints limits. These results are tabulated in **Table 6**.

Table 6: The parameters values for the three candidate points

Parameter number	Candidate result 1	Candidate result 2	Candidate result 3
1	0.0657 (m)	0.06657 (m)	0.06905 (m)
2	0.0661 (m)	0.06146 (m)	0.06278 (m)
3	0.076 (m)	0.079 (m)	0.08526 (m)
4	0.08474 (m)	0.082554 (m)	0.078586 (m)
5	0.11375 (m)	0.11914 (m)	0.11197 (m)
6	0.11379 (m)	0.11756 (m)	0.1032 (m)
7	0.06814 (m)	0.682 (m)	0.08209 (m)
8	0.06825 (m)	0.6815 (m)	0.07674 (m)
9	0.11822 (m)	0.11864 (m)	0.14807 (m)
10	0.08698 (m)	0.7748 (m)	0.0879 (m)
11	0.07785 (m)	0.7842 (m)	0.08572 (m)
12	0.1627997 (m)	0.15549 (m)	0.15574 (m)

Figure 11 illustrates the candidate results with the constraints.

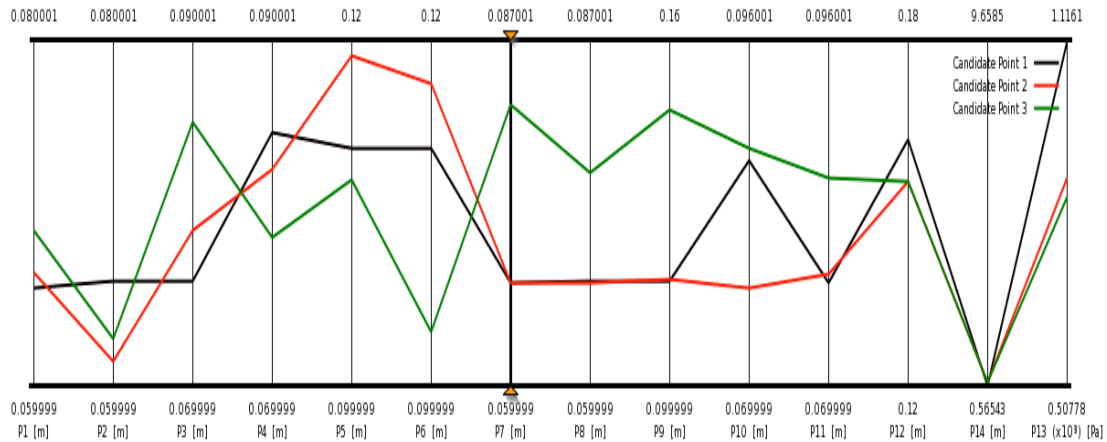


Figure 11: The candidate points

The lower horizontal axis represents the input parameters and the design variables and the upper horizontal axis represents the Von Misses stresses. The maximum value of Von Misses stresses is $(1.1161 \times 10^8 \text{ Pa})$. The first candidate result is used to apply the shell thickness optimization to reach the optimum solution. The upper, lower and side shells are used as design variables.

$$W_s^L \leq W_s \leq W_s^u, \quad i = 1, 2, \dots, 6 \tag{16}$$

Where, (W_s) represents the shell thickness for upper, lower and side shells respectively, (W_s^L) represents the lower bound and (W_s^u) represents the upper bound. The objective function is the same in stage 1. The values of the shell thicknesses before and after optimization are shown in **Table 7**.

Table 7: Shell parameters values before and after optimization

Parameter number	Original value	Optimized value
T1	0.006 (m)	0.006 (m)
T2	0.004 (m)	0.002 (m)
T3	0.004 (m)	0.002 (m)
T4	0.004 (m)	0.002 (m)
T5	0.004 (m)	0.002 (m)
T6	0.004 (m)	0.002 (m)

The thickness of the upper deck is not reduced as the stresses would increase. The lower and side shells are reduced. Figure illustrates the difference of weight before and after optimization.



Figure 12: The comparison between weight before and after optimization

The optimization process of the ferry under the studied constraints and objective function reduces the weight to be optimum with a reduction of 24.7% from the original weight. The total deformation is also improved due to the reduction of weight. **Figure 13** shows the comparison of the total deformation before and after optimization.

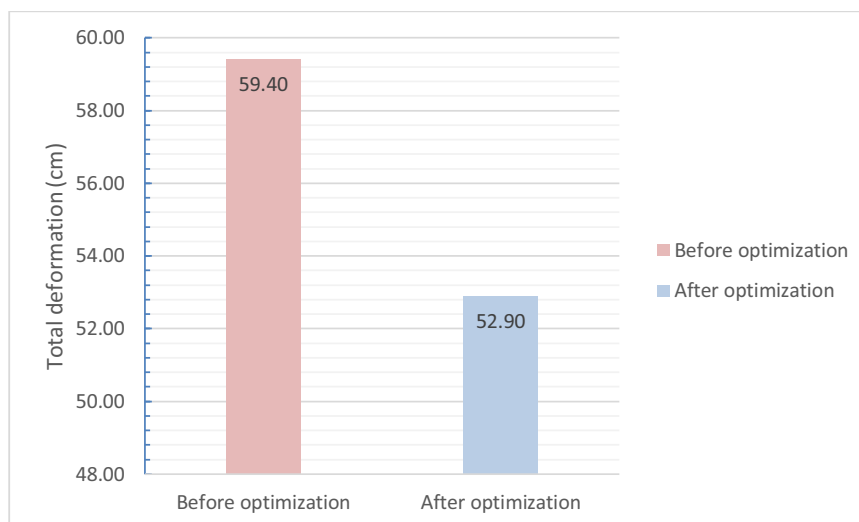


Figure 13: The comparison of total deformation

This chart illustrates that the buoyancy factor is minimized that results in the reduction of the ferry weight and the total deformation. It also illustrates that the effective constraint is the strength of the used material not the draft. If the material is changed with another one with a higher strength there will be better optimization results and more reduction in weight and cost of the ferry.

8. The redesign of the ferry

It is obvious that using material with more strength for the ferry results in more reduction in cross sections that result in further weight optimization. Different grades of the structural steel are used instead of steel 37 in addition to both the hybrid materials and the aluminium alloy (Al 6061) [38] also for the simulation of the ferry. The hybrid design is composed of the original steel stiffeners without

optimization covered with aluminium sheets from all sides. This hybrid design reduces the weight in addition to the simplification of the manufacturing process. The properties of the used materials are shown in **Table 8**.

Table 8: The properties of the used materials

	Steel 44	Steel 52	Al 6061
Density	7850 kg/m ³	7850 kg/m ³	2770 kg/m ³
Tensile yield strength	2.8 × 10 ⁸ (Pa)	3.6 × 10 ⁸ (Pa)	2.8 × 10 ⁸ (Pa)
Compressive yield strength	2.8 × 10 ⁸ (Pa)	3.6 × 10 ⁸ (Pa)	2.8 × 10 ⁸ (Pa)
Tensile ultimate strength	3.6 × 10 ⁸ (Pa)	4.6 × 10 ⁸ (Pa)	3.1 × 10 ⁸ (Pa)

The material is changed in the model and the new constraints values are determined for every material. The new values of the constraints are the yield strength values for the used materials.

Figure 14 shows the comparison between the ferry weight for the used materials after optimization and the original weight of the ferry.

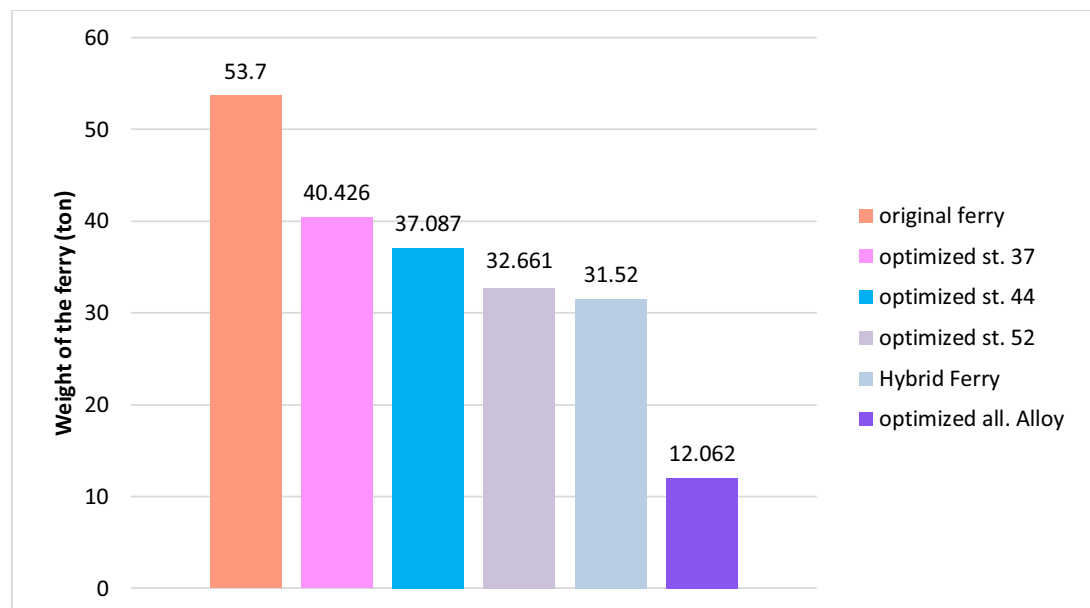


Figure 14: The Weight before and after optimization with different materials

For steel 37 the reduction in weight is about 24.7% as shown in **Figure 12**. For steel 44 the reduction of weight is about 30.9% of the original load, for steel 52 the reduction of weight is about 39.2% of the original load, for the hybrid design the reduction of weight is about 41.3% and for aluminium alloy the reduction of weight is about 77.5% of the original weight. This optimization values reduce the buoyancy factor and make it possible to increase the capacity of the ferry. This optimization values affect the total deformation as shown in **Figure 15**.

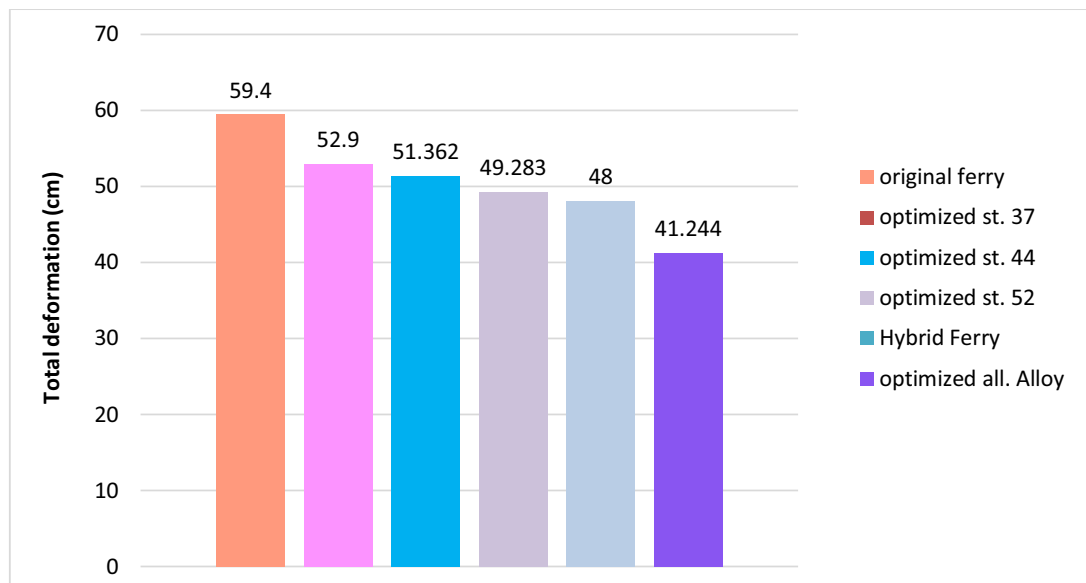


Figure 15: Total deformation before and after optimization with different materials

The deformation values are reduced as the total weight of the ferry is reduced.

9. Conclusion

In this study, the considered metallic ferry is simulated using ANSYS software. The ferry is loaded with a tank load (MLC-70). The model is verified with both practical and mathematical results. Optimization process is performed to obtain the minimum buoyancy factor and the optimum weight. Based on the aforementioned results, the buoyancy factor of the ferry is minimized and the ferry weight is reduced with a percentage of (24.7%) of the original weight for steel 37. Changing the grade of the structural steel to become steel 44 results in a reduction in weight of about (30.9%) of the original weight. The reduction in weight for steel 52 equals (39.2%) of the original weight. The hybrid design reduced the weight by about 41.3% from the original weight. Using aluminium alloy (Al 6061) instead of steel 37 results in a reduction of about (77.5%) of the original weight. Additionally, the total deformations are reduced for the whole optimized cases due to the reduction in weight. The strength of the used material has the effective constraint so, increasing the strength of the used material results in increasing the strength of the material and results in more reduction in weight.

References

1. Watanabe, E. and T. Utsunomiya, *Analysis and design of floating bridges*. Progress in Structural Engineering and Materials, 2003. **5**(3): p. 127-144.
2. Watanabe, E. and T. Utsunomiya, *Analysis and design of floating bridges*. Prog. Struct. Engng Mater, 2003: p. 127-144.
3. Zhang, J., et al., *Analytical Models of Floating Bridges Subjected by Moving Loads for Different Water Depths*. Journal of Hydrodynamics, Ser. B, 2008. **20**(5): p. 537-546.
4. Zhang, J., et al. *Simulation of a discrete pontoon floating bridge induced by moving loads*. in *Mechanics and Architectural Design: Proceedings of 2016 International Conference*. 2017. World Scientific.
5. Kim, T., et al., *A Study on Motion Control of Multiple Floating Units*.

6. Wu, J.-S. and P.-Y. Shih, *Moving-load-induced vibrations of a moored floating bridge*. Computers & structures, 1998. **66**(4): p. 435-461.
7. Shahrabi, M. and K. Bargi, *Numerical simulation of multi-body floating piers to investigate pontoon stability*. Frontiers of Structural and Civil Engineering, 2013. **7**(3): p. 325-331.
8. Khalifa, Y.A., *Study the structural system effect on the stability of floating metallic bridges*. 2008.
9. Erdal, O. and F.O. Sonmez, *Optimum Design of Composite Laminates for Maximum Buckling Load Capacity Using Simulated Annealing*. Composite Structures, 2005. **71**(1): p. 45-52.
10. Fu, S. and W. Cui, *Dynamic responses of a ribbon floating bridge under moving loads*. Marine Structures, 2012. **29**(1): p. 246-256.
11. Sun, J., et al., *An experimental investigation on the nonlinear hydroelastic response of a pontoon-type floating bridge under regular wave action*. SHIPS AND OFFSHORE STRUCTURES,, 2018. **13**: p. 233-243.
12. Hirono, Y., et al. *Positional displacement measurement of floating units based on aerial images for pontoon bridges*. in *International Conference on Advanced Engineering Theory and Applications*. 2016. Springer.
13. Cheng, Z., Z. Gao, and T. Moan, *Numerical Modeling and Dynamic Analysis of a Floating Bridge Subjected to Wind, Wave, and Current Loads*. Journal of Offshore Mechanics and Arctic Engineering, 2019. **141**(1): p. 011601.
14. Lie, H., et al. *Numerical modelling of floating and submerged bridges subjected to wave, current and wind*. in *ASME 2016 35th International Conference on Ocean, Offshore and Arctic Engineering*. 2016. American Society of Mechanical Engineers.
15. Sha, Y., et al., *Numerical investigations of the dynamic response of a floating bridge under environmental loadings*. Ships and Offshore Structures, 2018. **13**(sup1): p. 113-126.
16. Salem, A.I., *Weight and cost multi-objective optimization of hybrid composite sandwich structures*. 2016, University of Dayton.
17. rey Horn, J., N. Nafpliotis, and D.E. Goldberg. *A niched Pareto genetic algorithm for multiobjective optimization*. in *Proceedings of the first IEEE conference on evolutionary computation, IEEE world congress on computational intelligence*. 1994. Citeseer.
18. Zitzler, E. and L. Thiele, *An evolutionary algorithm for multiobjective optimization: The strength pareto approach*. TIK-report, 1998. **43**.
19. Corne, D.W., J.D. Knowles, and M.J. Oates. *The Pareto envelope-based selection algorithm for multiobjective optimization*. in *International conference on parallel problem solving from nature*. 2000. Springer.
20. Törn, A. and A. Žilinskas, *Global optimization*. Vol. 350. 1989: Springer.
21. Coello, C.A.C., *A comprehensive survey of evolutionary-based multiobjective optimization techniques*. Knowledge and Information systems, 1999. **1**(3): p. 269-308.
22. Koumoussis, V.K. and S. Arsenis, *Genetic algorithms in optimal detailed design of reinforced concrete members*. Computer - Aided Civil and Infrastructure Engineering, 1998. **13**(1): p. 43-52.
23. KIM, H. and H. ADELI, *Discrete cost optimization of composite floors using a floating-point genetic algorithm*. Engineering Optimization, 2001. **33**(4): p. 485-501.
24. Rigo, P. and C. Fleury, *Scantling optimization based on convex linearizations and a dual approach—Part II*. Marine structures, 2001. **14**(6): p. 631-649.
25. Shafieefar, M. and A. Rezvani, *Mooring optimization of floating platforms using a genetic algorithm*. Ocean Engineering, 2007. **34**(10): p. 1413-1421.
26. Brommundt, M., et al., *Mooring system optimization for floating wind turbines using frequency domain analysis*. Energy Procedia, 2012. **24**: p. 289-296.

27. Fathallah, E., et al., *Design optimization of lay-up and composite material system to achieve minimum buoyancy factor for composite elliptical submersible pressure hull*. Composite Structures, 2015. **121**: p. 16-26.
28. Fathallah, E., et al., *Multi-Objective Optimization of Composite Elliptical Submersible Pressure Hull for Minimize the Buoyancy Factor and Maximize Buckling Load Capacity*. Applied Mechanics and Materials, 2014. **578**: p. 75-82.
29. Russell, B.R., et al., *Reconceptualization and optimization of a rapidly deployable floating causeway*. Journal of Bridge Engineering, 2013. **19**(4): p. 04013013.
30. ANSYS, Inc. *Products Release 19.0*. 2019.
31. King, R., *Principles of flotation*. 1982: South African Institute of Mining and Metallurgy Johannesburg.
32. ANSYS, Inc. *Release Notes*. 2018.
33. Collins, L.M., et al., *A strategy for optimizing and evaluating behavioral interventions*. Annals of Behavioral Medicine, 2005. **30**(1): p. 65-73.
34. Collins, L.M., S.A. Murphy, and V. Strecher, *The multiphase optimization strategy (MOST) and the sequential multiple assignment randomized trial (SMART): new methods for more potent eHealth interventions*. American journal of preventive medicine, 2007. **32**(5): p. S112-S118.
35. Elsayed, F., et al. *Optimal Design Analysis of Composite Submersible Pressure Hull*. in *Applied Mechanics and Materials*. 2014. Trans Tech Publ.
36. Helal, M., et al., *Numerical Analysis of Sandwich Composite Deep Submarine Pressure Hull Considering Failure Criteria*. Journal of Marine Science and Engineering, 2019. **7**(10): p. 377.
37. Fathallah, E., *Finite Element Modelling and Multi-Objective Optimization of Composite Submarine Pressure Hull Subjected to Hydrostatic Pressure*. Materials Science Forum, 2019. **953**: p. 53-58.
38. Hellier, A., P. Chaphalkar, and G. Prusty, *Fracture Toughness Measurement for Aluminium 6061-T6 using Notched Round Bars*. 2017.